A non-inverting single-switch buck-boost converter based LED driver

Devi Maheswaran[1], Sreedevi Vellithiruthi Thazhathu[2], Deepa Thangavelusamy[1]
[1]School of Electrical Engineering, Vellore Institute of Technology, Chennai, India
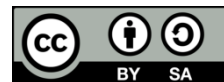[2]Centre for Smart Grid Technologies, School of Electrical Engineering, Vellore Institute of Technology, Chennai, India

Article Info

ABSTRACT

This paper focuses on a single-switch buck-boost (SSBB) converter for light emitting diode (LED) lighting applications. The proposed LED driver with power factor correction (PFC) shows enhanced performance in terms of input power factor, efficiency and reduced voltage stress across the switch. The presented LED driver is operated in discontinuous conduction mode (DCM). The input PFC is carried out using average current mode control (ACMC) and the controller is optimized using artificial bee colony (ABC) algorithm. A hardware prototype of 50W LED driver with ACMC for PFC is implemented using a programmable interface circuit (PIC) microcontroller. The experimental results are presented and the performance is compared with a conventional buck boost LED driver. The proposed SSBB LED driver achieves an input power factor of 0.96 with an efficiency of 98%.

Corresponding Author:

Sreedevi Vellithiruthi Thazhathu
Centre for Smart Grid Technologies, School of Electrical Engineering, Vellore Institute of Technology
Chennai, Tamil Nadu, India
Email: sreedevi.vt@vit.ac.in

1. INTRODUCTION

The solid state lighting (SSL) technology replaces traditional lighting solution for the past few years [1]–[3]. At present high brightness light emitting diodes (HBLEDs) are very attractive light sources due to their excellent characteristics such as: long life span, mercury free construction, energy efficiency, fast response, environmental friendliness, and solid state encapsulation [4]–[7]. The LED technology was previously used for status indicators, board level electronic systems and transport signals [8]. But recently, it has been considered as a viable solution in display, decorative and general lighting [9]. The worldwide report shows that nearly 30% of total energy consumed is spent on buildings [10]. Since lighting accounts for a major share of energy consumption worldwide, it is the need of the hour to look for energy efficient LED lighting system. Due to the VI characteristics of LEDs, controlling its dc forward current requires an LED driver. Since the primary energy source is ac, there is a need for an AC/DC converter to be placed between the supply and HBLEDs [10]. If the total power handled by these converters is greater than 25 W, then the harmonic content of line current must comply with lighting standards such as IEC61000 3.2 and ENERGYSTAR 2009. To comply with these regulations, the only practical method is to use active power factor correction (PFC) converters [10], [11].

Active LED driver circuits incorporate switched mode power conversion topology. It takes the advantages of high frequency operation and active output current regulation with compactness. These advantages make the active type LED drivers very distinctive for a broad range of interior applications [12]. The various functions like power factor correction (PFC), current distribution, dimmable lighting, isolation, fault prevention and temperature maintenance can be easily included in switched mode based LED circuits to meet

diverse applications [13]–[15]. Among the switched mode circuits, a buck PFC circuit is commonly used because of its simplicity. The output voltage of buck circuit will be lesser than the input voltage. It faces dead zone which means that, when input voltage is lesser than the output voltage, the input current reaches zero. This leads to distortions in source current [13]. Hence, buck type circuits are not suitable for PFC applications. The boost circuit is suitable for PFC applications for LED lighting due to its source side inductor [13], [15], [16]. It suffers from higher voltage stress and requires more number of LEDs to be connected in series. This leads to increased cost [17]. Flyback circuit is a good choice for low power applications due to less number of components. However, due to high leakage inductance, efficiency is low [18].

A traditional buck-boost circuit works in step-up/step-down mode and it is commonly used for low and medium LED power applications [19]–[21]. However, it suffers from high switching stress due to inverted output [22]–[25]. It requires isolated gate driver circuit and independent grounding for source and load side. A new approach for the design of proportional-integral-derivative (PID) controller in order to improve the performance of buck-boost LED driver is presented in [22]. A bridgeless buck-boost PFC circuit with isolated flyback operating in discontinuous conduction mode (DCM) is reported [23]. The design application of bridgeless buck-boost PFC circuit is well suited for wide range of LED lighting systems. Recently, a high-efficiency non-isolated zero voltage switching (ZVS) synchronous buck-boost LED driver for automobile lighting applications is also presented [24]. A non-inverting buck-boost (NIBB) converter incorporating two switches using electrolytic capacitor (EC)-less PFC integrated bi-directional converter (BDC) is available in the literature [25]. Due to the large number of active switches and devices, the circuit complexity increases in the case of two switch NIBB converter.

Hence, in this paper a non-inverting, single switch buck-boost (SSBB) circuit as LED driver is suggested to overcome the above-mentioned drawbacks. The voltage gain of the SSBB driver circuit is higher than the traditional buck–boost circuit [26]. Here, in this converter, only one power switch is employed which makes the control scheme simple as well as it reduces the switching power losses. The proposed SSBB LED driver circuit solves the above-mentioned problems of traditional buck boost circuits, by reducing the stress on the switch components. To implement PFC, average current mode control (ACMC) scheme is implemented. The controller parameters are optimized using the well-known artificial bee colony (ABC) algorithm so that the input power factor is almost unity. The efficiency of the proposed LED driver is almost 98%, due to the reduced switch stress as well as single switch operation.

The remaining part of the paper is organized in this way. Section 2 presents circuit configuration and principle of operation of the proposed LED driver. The design of the SSBB LED driver in DCM is discussed in section 3. Section 4 focuses on state space modelling, ACMC technique and ABC algorithm for tuning the controllers and finally, section 5 discusses the simulation and experimental results of the SSBB LED driver system.

2.   CIRCUIT CONFIGURATION AND PRINCIPLE OF OPERATION OF SSBB LED DRIVER

The block diagram implementation of the SSBB LED driver is shown in Figure 1. It consists of a diode bridge rectifier, non-inverting SSBB converter, input PFC controller and LED load. The SSBB converter consists of a single switch (S), two diodes (D_a, D_b), five energy storage elements including inductors and capacitors (L_a, L_b, C_a, C_b and C_c) as shown in Figure 1. Among the passive elements, capacitors (C_a and C_b) are in parallel with the diodes (D_a and D_b). The input current shaping of the proposed LED driver circuit is carried out by ACMC. ACMC scheme employs an outer voltage loop and an inner current loop as shown in Figure 1.
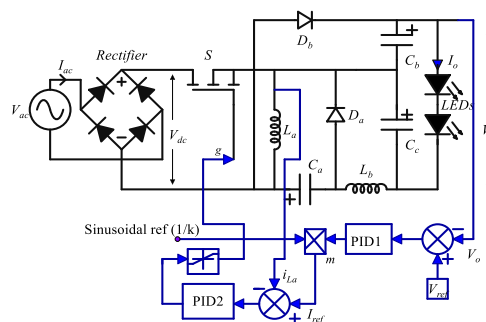

Figure 1. SSBB LED driver with ACMC

The proposed SSBB LED driver circuit operates in DCM. The theoretical waveforms of the SSBB converter are depicted in Figure 2 [26]. The modes of operation of SSBB are depicted in Figures 3(a) to 3(e).

During mode I (time interval: t_0 to t_1 as seen in Figure 2), when the switch (S) is ON, both the diodes (D_a and D_b) are in OFF condition. As seen in Figure 3(a), the inductance (L_a) is energized through (V_{dc}) and the inductance (L_b) is also magnetized by capacitors (C_a and C_c) via V_{dc}. Hence energy stored in the capacitors (C_b and C_c) are discharged through the LEDs. The voltages across the inductors, (V_{La} and V_{Lb}) are given by (1) and (2).

$$V_{La} = V_{dc} \tag{1}$$

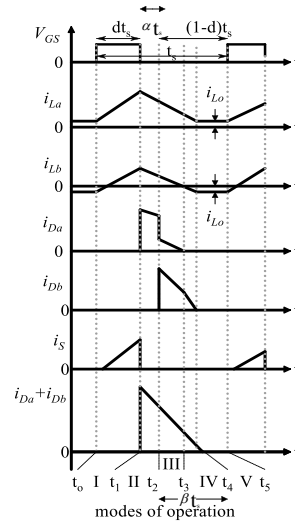$$V_{La} = V_{dc} + V_{Ca} - V_{Cc} \tag{2}$$

Figure 2. Theoretical waveforms of SSBB LED driver in DCM

During mode II (time interval: t_1 to t_2 as seen in Figure 2), when switch (S) is turned OFF, diode (D_a) is turned ON and diode (D_b) is still in OFF condition. As seen in Figure 3(b), the capacitors (C_a and C_c) are charged through inductance (L_a and L_b) respectively. The inductors are demagnetized and the energy stored in the capacitor (C_b) is discharged through the LEDs. Hence voltage across the inductors, (V_{La} and V_{Lb}) are given by (3) and (4).

$$V_{La} + V_{dc} = 0 \tag{3}$$

$$V_{Lb} = -V_{Cc} \tag{4}$$

Capacitors (C_a and C_b) are charged and discharged respectively, until their voltages are equal. Therefore, the capacitors (C_a and C_c) are not connected in parallel due to different voltage levels across them. Hence, the current spikes are avoided through the diodes and capacitors in this mode of operation.

During mode III (time interval: t_2 to t_3 as seen in Figure 2), the switch (S) is still in OFF condition and the diodes (D_a and D_b) are in ON condition as noticed in Figure 3(c). The voltage across the capacitors (C_a and C_b) are equal as mentioned in mode I operation which are given by (1) and (2). Hence, the capacitors (C_a and C_b) are in parallel. The voltages across the capacitors (C_a and C_b) are mentioned in (5).

$$V_{Ca} = V_{Cb} \tag{5}$$

These capacitors (C_a and C_b) are charged through L_a. Also, L_b charges the capacitor (C_c). Hence inductors (L_a and L_b) are demagnetized linearly. During mode IV (time interval: t_3 to t_4 as seen in Figure 2), when switch (S) is still in OFF condition, the diode (D_a) remains OFF and the diode (D_b) in ON state as noticed from Figure 3(d). The (3) and (4) are valid for mode IV.

During mode V (time interval: t_4 to t_5 as seen in Figure 2), when switch (S) and the diodes (D_a and D_b) are all in OFF condition as noticed in Figure 3(e). The current through inductance will be constant and hence the voltage across the inductance will be zero as represented by (6).

$$V_{La} = V_{Lb} = 0 \tag{6}$$

The voltage across capacitors (C_b and C_c) is $\frac{d}{1-d}$ times the rectified dc input voltage (V_{dc}), where d is the duty cycle. Since LED load is connected across the capacitors (C_b and C_c), the output voltage (V_o) is equal to $\frac{2d}{1-d}$ times of V_{dc}.
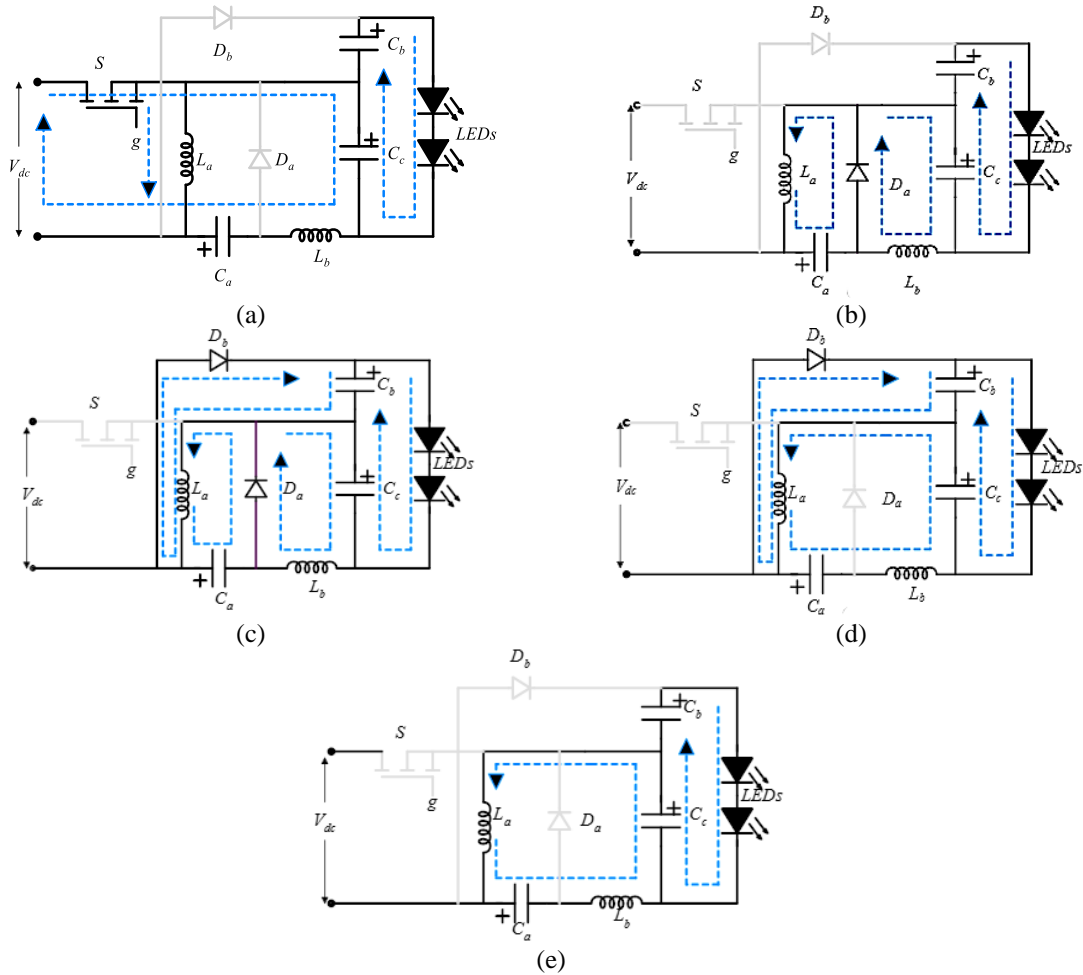

Figure 3. Operating modes of SSBB converter (a) mode I, (b) mode II, (c) mode III, (d) mode IV, and (e) mode V

3.   DESIGN OF SSBB LED DRIVER IN DCM

Under steady state operation and applying the volt second balance equation on inductance (L_a) and using (1), (3), and (4), the following (7) is obtained.

$$V_{L_a} = dV_{dc} - (\alpha + \beta)V_{Ca} = 0 \tag{7}$$

Where αt_s represents the time interval of second mode of operation and βt_s represents the time interval of third and fourth modes of operation as shown in Figure 2. By simplifying (7), we get (8).

$$V_{Ca} = \frac{d}{\alpha+\beta} V_{dc} \tag{8}$$

Using (5) and (8), the voltage gain (G_v) in DCM is derived as (9).

$$G_{(V)DCM} = \frac{2d}{\alpha+\beta} \tag{9}$$

For $t = d_{t_s}$, $t_0 = 0$, as seen in Figure 2 the current ripple of the inductors (L_a and L_b) is obtained as Δi_{L_a} and Δi_{L_b}.

$$\Delta i_{La} = \frac{d(V_{dc})}{f_{sw} L_a} \tag{10}$$

$$\Delta i_{Lb} = \frac{d(V_{dc})}{f_{sw} L_b} \tag{11}$$

According to the waveforms noticed from Figure 2, the average current values through the inductances (L_a and L_b) can be written as follows:

$$i_{L_a} = \frac{d+\alpha+\beta}{2} \Delta i_{L_a} + I_{L_O} \tag{12}$$

$$i_{L_b} = \frac{d+\alpha+\beta}{2} \Delta i_{L_b} + I_{L_O} \tag{13}$$

where (I_{LO}) is the inductor current gain in DCM mode, from (10), (11), (12) and (13), it is derived as (14).

$$I_{L_O} = \frac{V_{dc}d}{f_{sw}} \left[\left(\left(\frac{d+\alpha+\beta}{2} \right) - \frac{\alpha+\beta}{4} \right) \frac{1}{L_b} - \frac{\alpha+\beta}{4L_a} \right] \tag{14}$$

During DCM, the currents flowing from inductors do not reach zero. However, they reach I_{L_O} as seen in Figure 2. Substituting (12) and (13) into (14) yields (15) and (16). Hence:

$$i_{Lb} = I_O = \frac{V_O}{R_L} \qquad V_{Ca} = \frac{d}{\alpha+\beta} V_{dc} \qquad V_{Ca} = \frac{d}{\alpha+\beta} V_{dc} \qquad V_{Ca} = \frac{d}{\alpha+\beta} V_{dc} \qquad V_{Ca} = \frac{d}{\alpha+\beta} V_{dc} \tag{15}$$

where R_L, is the equivalent resistance of LED load. The inductance current, (i_{Lb}) can also be written as (16).

$$i_{Lb} = \frac{V_{dc}d}{f_{sw} L_b} \left(\frac{d+\alpha+\beta}{2} \right) - \frac{V_{dc} \, d}{f_{sw}} \left[\left(\left(\frac{d+\alpha+\beta}{2} \right) - \frac{\alpha+\beta}{4} \right) \frac{1}{L_b} - \frac{\alpha+\beta}{4L_a} \right] \tag{16}$$

Where:

$$\alpha+\beta = \sqrt{\frac{8 f_{sw} (L_a \| L_b)}{R_L}} \tag{17}$$

using (9) and (17), the voltage gain (G_v) in DCM of the SSBB converter can be written as (18).

$$G_{(V)DCM} = \frac{2d}{\sqrt{\dfrac{8 f_{sw} (L_a \| L_b)}{R_L}}} \tag{18}$$

It is noticed that when average currents of diodes are <50 % of current ripple, the diodes are turned OFF. This is stated in (19).

$$i_{L_a} + i_{L_b} < \Delta i_{L_a} + \Delta i_{L_b} \tag{19}$$

By considering all the inductances, the simplified inductor time constant (τ_L) is obtained by substituting current ripples of inductors from (10) and (11) into (19) as (20).

$$\tau_L = \frac{4 f_{sw} (L_a \| L_b)}{R_L} \tag{20}$$

Hence the voltage gain of the LED driver in DCM will be re-written by substituting (20) in (18) as (21).

$$G_{(V)DCM} = \frac{2d}{\sqrt{2\tau_L}} \qquad (21)$$

The boundary normalized inductor current (τ_{LB}) is obtained from the gain of the SSBB converter.

$$\tau_{LB} = (1/2))^2 \qquad (22)$$

When $\tau_L < \tau_{LB}$, SSBB converter works in DCM, but if $\tau_L > \tau_{LB}$, the SSBB converter switches over to CCM. The values of inductors are obtained from (20) and (22). The capacitors (C_a, C_b and C_c) are designed to reduce the output voltage ripple. The design equations are mentioned below:

$$C_a \geq d\, V_o / f_{sw} R_L \Delta V_{Ca} \qquad (23)$$

$$C_b \geq 2d^2/(1-d) f_{sw} R_L L_b \Delta V_{Cb} \qquad (24)$$

$$C_c \geq d^2 V_{dc} / f_{sw}^2 L_b \Delta V_{Cc} \qquad (25)$$

where ΔV_{ca}, ΔV_{cb}, ΔV_{cc} are the ripple voltages across the capacitors (C_a, C_b and C_c).

4. CONTROL METHODOLOGY
4.1. ACMC scheme for PFC
As stated in the circuit configuration of section 2, the ACMC scheme for PFC includes an inner current loop and an outer voltage loop. In the outer voltage loop, the load voltage (V_o) is sensed and it is compared with (V_{ref}) to generate the voltage error signal (e_1). Then, the voltage error signal (e_1) is processed by PID1 and the output of PID1 is multiplied (m) with the rectified dc voltage to provide reference current (I_{ref}) as shown in Figure 4. In the inner loop, the sensed inductor current (i_{La}) is compared with I_{ref} to produce current error signal (e_2), which will be processed by PID2. Since the output of PID2 signal is analog in nature, the current error signal obtained from the inner current loop is fed as the input to the PWM comparator (c). It is then compared with the ramp signal (V_{ramp}) and fed to the PWM latch, to generate gate pulses to the switch (S). The parameters of PID 1 and 2 are obtained by employing a meta-heuristic optimization algorithm known as artificial bee colony (ABC) [27]–[29]. State space modelling of SSBB converter is necessary to obtain the optimized values of PID controllers [30]–[33].

4.2. State space modelling of the SSBB LED driver circuit
The proposed LED driver circuit is modelled using state space approach [30]–[33]. The SSBB converter when operated in DCM, exhibits five different modes in one switching period (t_s). The analytical waveforms of the SSBB converter are depicted in Figure 2. The general state-space equations for these five modes are represented by (26) to (30).

$$\left.\begin{array}{l} \dot{X} = A_1 X + B_1 U \\ Y = C_1 X + E_1 U \end{array}\right\} \qquad (26)$$

$$\left.\begin{array}{l} \dot{X} = A_2 X + B_2 U \\ Y = C_2 X + E_2 U \end{array}\right\} \qquad (27)$$

$$\left.\begin{array}{l} \dot{X} = A_3 X + B_3 U \\ Y = C_3 X + E_3 U \end{array}\right\} \qquad (28)$$

$$\left.\begin{array}{l} \dot{X} = A_4 X + B_4 U \\ Y = C_4 X + E_4 U \end{array}\right\} \qquad (29)$$

$$\left.\begin{array}{l} \dot{X} = A_5 X + B_5 U \\ Y = C_5 X + E_5 U \end{array}\right\} \qquad (30)$$

Where A, B, C, E are the system matrix, X is the state variable, $\dot{X}$ is the state variable derivative, U is the input and Y is the output. Since the SSBB LED driver consists of La, Lb, Ca, Cb and Cc the state vector variables selected are as given by (31).

$$x_1 = i_{L_a} , \ x_2 = i_{L_b} , \ x_3 = v_{C_a} , x_4 = v_{C_b} , x_5 = v_{C_c} \tag{31}$$

From (26) to (30), the resultant state space equation can be written as mentioned in (32).

$$\left. \begin{array}{l} \dot{X} = AX + BU \\ Y = CX + EU \end{array} \right\} \tag{32}$$

By considering the duty cycles of each state as (d1, d2, d3, d4, d5), the matrices can be expressed as in (33) to (36).

$$A = A_1 d_1 + A_2 d_2 + A_3 d_3 + A_4 d_4 + A_5 d_5 \tag{33}$$

$$B = B_1 d_1 + B_2 d_2 + B_3 d_3 + B_4 d_4 + B_5 d_5 \tag{34}$$

$$C = C_1 d_1 + C_2 d_2 + C_3 d_3 + C_4 d_4 + C_5 d_5 \tag{35}$$

$$E = E_1 d_1 + E_2 d_2 + E_3 d_3 + E_4 d_4 + E_5 d_5 \tag{36}$$

Where, E represents the feed forward gain matrix and it is assumed to be zero and the duty cycles of each state can be expressed in (37) to (40) by looking into the Figure 2.

$$d_1 = d \, t_s \tag{37}$$

$$d_2 = \alpha \, t_s \tag{38}$$

$$d_3 + d_4 = \beta \, t_s \tag{39}$$

$$d_5 = (1 - d) \, t_s - \beta \, t_s \tag{40}$$

The matrices A_1, A_2, A_3, A_4, A_5, B_1, B_2, B_3, B_4, B_5, C_1, C_2, C_3, C_4, C_5 are determined from the equivalent circuits mentioned in Figure 3 and are presented in (41) to (47).

$$A_1 = \begin{vmatrix} 0 & 0 & 0 & 0 & 0 \\ 0 & 0 & \dfrac{1}{L_b} & 0 & -\dfrac{1}{L_b} \\ 0 & -\dfrac{1}{C_a} & 0 & 0 & 0 \\ 0 & 0 & 0 & -\dfrac{1}{C_b R_L} & -\dfrac{1}{C_b R_L} \\ 0 & \dfrac{1}{C_c} & 0 & -\dfrac{1}{R_L C_c} & -\dfrac{1}{R_L C_c} \end{vmatrix} \tag{41}$$

$$A_2 = \begin{vmatrix} 0 & 0 & -\dfrac{1}{L_a} & 0 & 0 \\ 0 & 0 & 0 & 0 & -\dfrac{1}{L_b} \\ \dfrac{1}{C_a} & 0 & 0 & 0 & 0 \\ 0 & 0 & 0 & \dfrac{1}{C_b R_L} & -\dfrac{1}{C_b R_L} \\ 0 & \dfrac{1}{C_c} & 0 & -\dfrac{1}{R_L C_c} & -\dfrac{1}{R_L C_c} \end{vmatrix} \tag{42}$$

$$A_3 = \begin{vmatrix} 0 & 0 & -\dfrac{1}{L_a} & 0 & 0 \\ 0 & 0 & 0 & 0 & \dfrac{1}{L_b} \\ \dfrac{1}{C_a+C_b} & 0 & 0 & -\dfrac{1}{R_L(C_a+C_b)} & -\dfrac{1}{R_L(C_a+C_b)} \\ \dfrac{1}{C_a+C_b} & 0 & 0 & -\dfrac{1}{R_L(C_a+C_b)} & -\dfrac{1}{R_L(C_a+C_b)} \\ 0 & -\dfrac{1}{C_c} & 0 & -\dfrac{1}{R_L C_c} & -\dfrac{1}{R_L C_c} \end{vmatrix} \tag{43}$$

$$A_4 = \begin{vmatrix} 0 & 0 & 1+\dfrac{L_a}{L_b} & -\dfrac{L_a}{L_b} & 1-\dfrac{L_a}{L_b} \\ 0 & 0 & \dfrac{1}{L_b} & -\dfrac{1}{L_b} & -\dfrac{1}{L_b} \\ 0 & -\dfrac{1}{C_a} & 0 & 0 & 0 \\ \dfrac{1}{C_b} & \dfrac{1}{C_b} & 0 & -\dfrac{1}{R_L\,C_b} & -\dfrac{1}{R_L\,C_b} \\ 0 & \dfrac{1}{C_c} & 0 & -\dfrac{1}{R_L C_c} & -\dfrac{1}{R_L C_c} \end{vmatrix} \tag{44}$$

$$A_5 = \begin{vmatrix} 0 & 0 & -\dfrac{1}{(L_a-L_b)} & 0 & \dfrac{1}{(L_a-L_b)} \\ 0 & 0 & -\dfrac{1}{(L_a-L_b)} & 0 & \dfrac{1}{(L_a-L_b)} \\ 0 & -\dfrac{1}{C_a} & 0 & 0 & 0 \\ 0 & 0 & 0 & -\dfrac{1}{R_L\,C_b} & -\dfrac{1}{R_L\,C_b} \\ -\dfrac{1}{C_c} & 0 & 0 & -\dfrac{1}{R_L C_c} & -\dfrac{1}{R_L C_c} \end{vmatrix} \tag{45}$$

$$B = \begin{vmatrix} \dfrac{1}{L_a} \\ \dfrac{1}{L_b} \\ 0 \\ 0 \\ 0 \end{vmatrix} \tag{46}$$

$$C = \begin{vmatrix} 0 & 0 & 0 & 1 & 1 \end{vmatrix} \tag{47}$$

By substituting the design values mentioned in Tables 1 and 2 in (33) to (36), the transfer function $(V_o(s)/V_{dc}(s))$ for the SSBB LED driver circuit is given by (48).

$$G(s) = \frac{1.28\ e^{06}s^2 + 1.64\ e^{09}s + 9.44\ e^{-05}}{s^4 + 898\ s^3 + 9\ e^{06}s^2 + 2.19\ e^{08}s + 3.07\ e^{10}} \tag{48}$$

Table 1. The specification details of SSBB LED driver

S.No.	Parameters	Values
1	Input ac voltage (V_{ac})	230 V
2	Output power (P_o)	50 W
3	Load voltage (V_o)	140 V
4	Load current (I_o)	350 mA
5	Switching frequency (f_{sw})	25 kHz

Table 2. The design values of elements of SSBB LED driver circuit

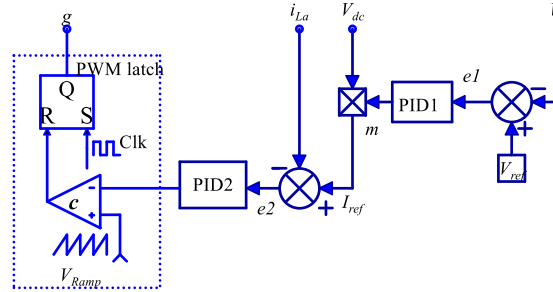| S.No.	Parameters	Values
1	Inductance (L$_a$, L$_b$)	1.7 *mH*, 5 *mH*
2	Capacitance (C$_a$, C$_b$, C$_c$)	10 µF, 1000 µF, 680 µF

Figure 4. ACMC scheme of SSBB LED driver

5.   SIMULATIONS AND EXPERIMENTAL RESULTS

The specifications of the SSBB LED driver are mentioned in Table 1. The designed values of the passive elements incorporated in the LED driver circuit are presented in Table 2. The simulation is carried out using PSIM software.

5.1. Tuning of PID controllers

The parameters of the PID controllers 1 and 2 are obtained by using the well-known ABC optimization algorithm. ABC algorithm is one of the established meta-heuristic methods. The ABC algorithm was introduced in 2005 [27], inspired by the intelligent foraging behavior of honey bee swarms. Each cycle of the ABC algorithm comprises three steps:
- Sending the employed bee to the possible food-source positions (solutions) and measuring their nectar amounts (fitness values).
- Onlookers selecting a food source after sharing the information from the employed bees in the previous step.
- Determining the scout bees and then sending them into entirely new food-source positions.
    The following are the constraints and objective functions used for tuning the PID controllers 1 and 2.
- To optimize PID1.
    The objective function is:

$$\text{minimize } f(\phi) = \int \left(V_{ref} - V_o \right)^2 dt$$

    subjected to the constraint d$_{min}$<d<d$_{max}$
- To optimize PID2.
    The objective function is:

$$\text{minimize } f(\phi) = \int \left(I_{ref} - i_{La} \right)^2 dt$$

    subjected to the constraint d$_{min}$<d<d$_{max}$

The parameters of the ABC algorithm for simulation are given in Table 3. The values of k$_p$, k$_i$ and k$_d$ obtained for both PID1 and PID2 are mentioned in Table 4. The time domain specifications for the transfer function $V_o(s)/V_{dc}(s)$ of SSBB LED driver circuit is presented in Table 5. It is noticed that the ABC algorithm based tuning offers reduced rise time, settling time and percentage peak overshoot.

Table 3. Parameters of ABC algorithm

Algorithm parameters	Values
Colony size	10
Employed bees	5
Food source	10
Max. iterations	23

Table 4. PID controller parameters using ABC for SSBB LED driver circuit

Controller parameters	PID 1	PID 2
k$_p$	1	0.1
k$_i$	0.3	0.3
k$_d$	0.1	1

Table 5. Time domain specifications of SSBB LED driver

S.No.	Time domain	Parameter values
1	Rise time (t_r)	0.00013 s
2	Peak overshoot (M_p)	9.8%
3	Setting time (t_s)	0.316 s
4	Final value (G_p)	1.1
5	Delay time (t_d)	0.0001 s

The closed loop poles are located at the following points given: 1.0e+03 *; -0.4370+2.9639i; 0.4370-2.9639i; 0.0120+0.0572i; 0.0120-0.0572i. All the poles are lying on the left half of s-plane. So, the single switch buck boost converter is stable. The closed loop frequency response of the proposed LED system is shown in Figure 5. From the bode diagram, it is noted that the gain margin is infinity and phase margin is 63.3°. The tuned response of the proposed LED system is found to be stable.
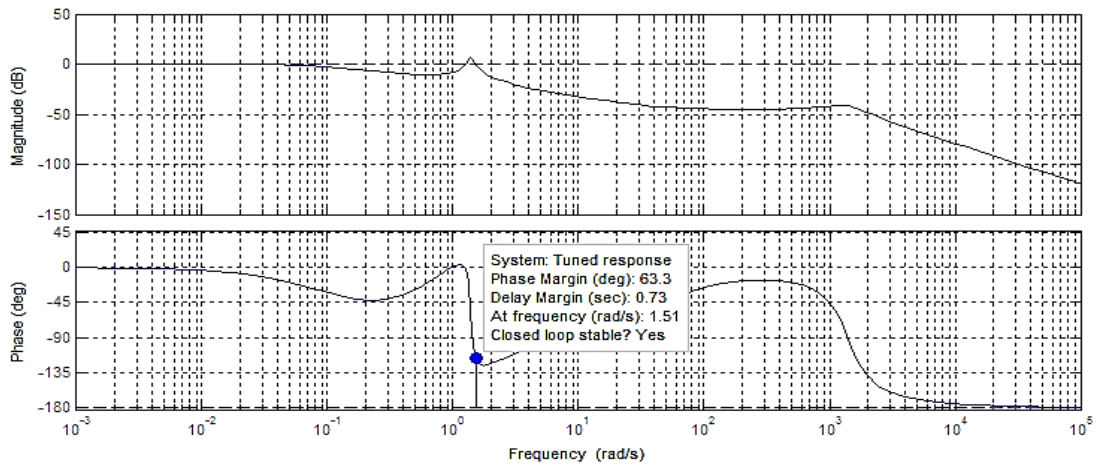
Figure 5. Bode plot of SSBB LED driver

5.2. Hardware setup of SSBB LED driver circuit

The practical implementation of the proposed LED driver with ACMC is shown in Figure 6. The prototype model of SSBB LED driver is implemented using a PIC microcontroller (16F877A). These are available in a 28/40 pin enhanced flash microcontrollers. It has enhanced peripherals for A/D conversion and PWM technique. The sensing of the output voltage (V_o) and the rectified dc voltage (V_{dc}) is done by the voltage sensors (LV25P). The inductor current (i_{La}) is sensed by the current sensor (HE025T01) and it is fed to the signal conditioning unit. The controller processes the control algorithm and through the driver circuit (IR250) generates the gate pulses to drive the switch (S). The photograph of the hardware setup is illustrated in Figure 7.
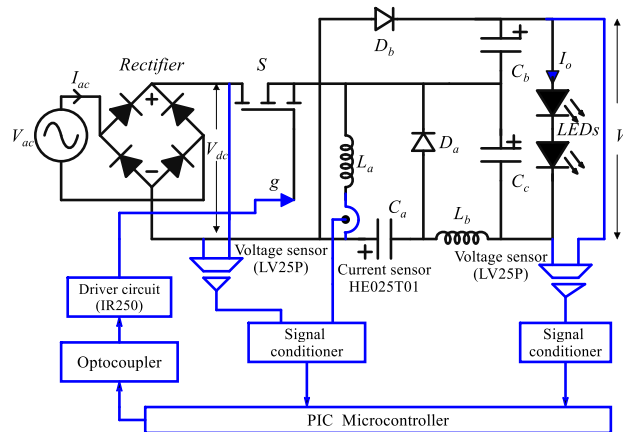

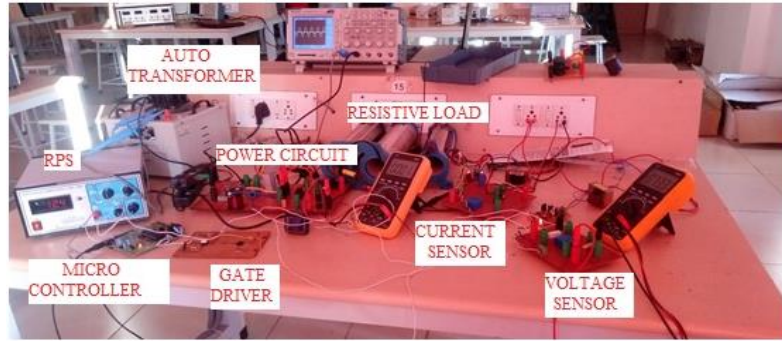Figure 6. Implementation of the SSBB LED driver with ACMC

Figure 7. Experimental setup of SSBB LED driver

The generation of gate pulses during simulation and experimental setup are depicted in Figures 8(a) and 8(b). The duty cycle is verified to be 0.25 with a switching frequency of 25 kHz. It can be observed from Figures 9(a) and 9(b), that the supply current (I_{ac}) is in phase with supply voltage (V_{ac}) during simulation and experimental setup. Hence the input power factor is nearly unity.
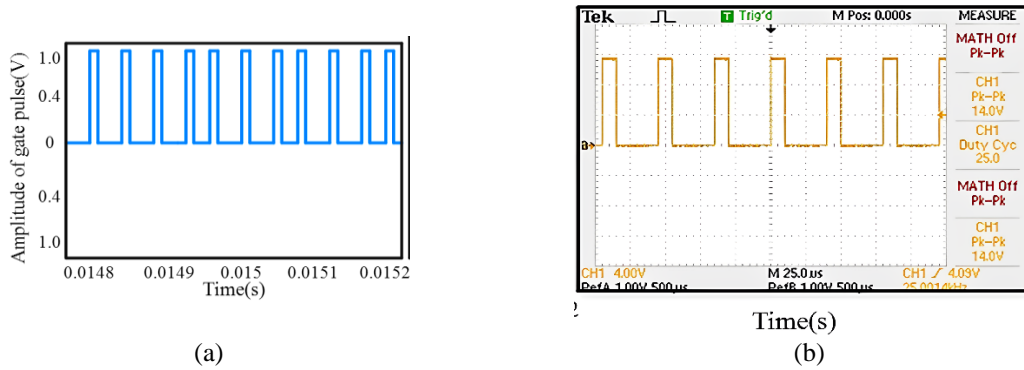

(a)	(b)

Figure 8. Waveforms of generated gate pulses (a) simulation results and (b) experimental results

(a)	(b)
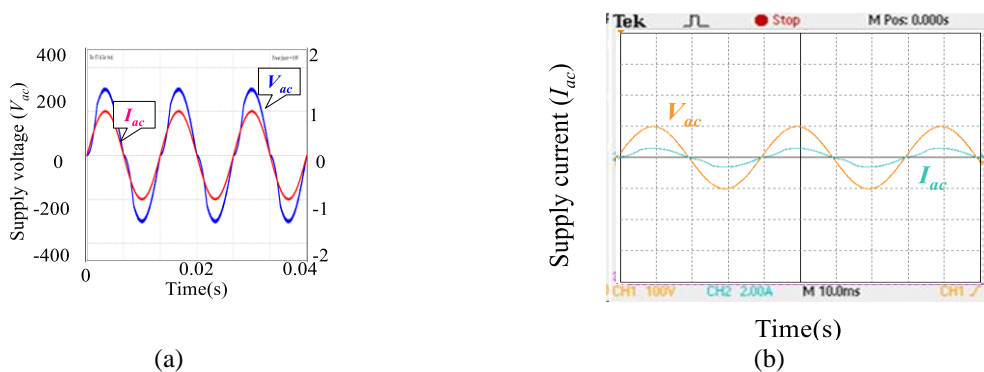
Figure 9. Supply voltage and supply current waveforms of SSBB LED driver (a) simulation results and (b) experimental results

The load voltage (V_o) and load current (I_o) waveforms of SSBB LED driver during simulation and experimental setup are illustrated in Figures 10(a) and 10(b). A load voltage (V_o) of 140 V and a load current (I_o) of 350 mA are obtained. The inductor current (i_{La} and i_{Lb}) waveforms are shown in Figure 11. It is seen from Figure 11 that the SSBB converter operates in DCM.
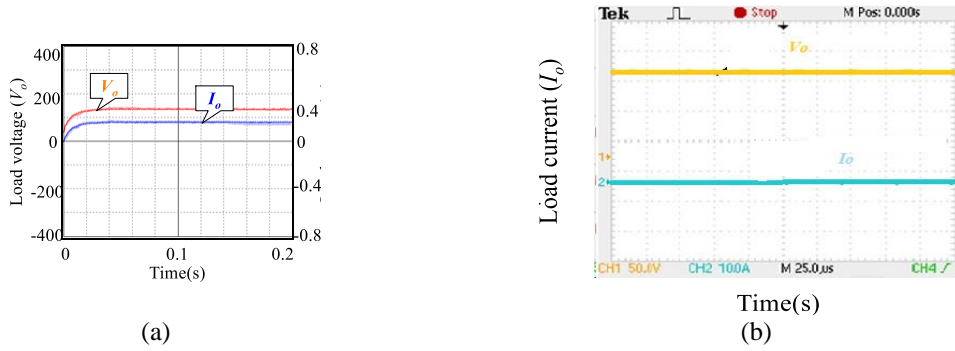
Figure 10. Load voltage and load current waveforms of SSBB LED driver (a) simulated results and
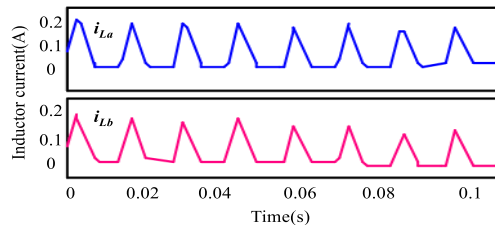(b) experimental results

Figure 11. Simulated waveforms of inductor currents during DCM

5.3. Performance comparison of SSBB LED driver circuit

The SSBB LED driver circuit is compared with a DSBB converter [25]. The DSBB converter also works in DCM. Both the circuits are simulated using same voltage and current parameters, as mentioned in Table 1. The voltage stress across various components of the circuit plays an important role in deciding the rating of diodes and switches. The voltage gain (G_v) equation and voltage stress across the switch for SSBB converter with respect to DSBB converter is given in Table 6.

The normalized voltage stress comparison graph is also presented in Figure 12(a). The SSBB LED driver circuit shows reduction in the voltage stress. The efficiency analysis of the proposed LED driver circuit for different load conditions is depicted in Figure 12(b). The efficiency curve depicts that the proposed converter has higher efficiency compared to the conventional buck-boost circuit. The performance superiority in terms of efficiency, input power factor and ripple in the output voltage is also discussed. The bar chart shown in Figure 13 depicts that the proposed LED driver circuit has an efficiency of 98%, input power factor of 0.96 and percentage ripple reduced by 5%.

Table 6. Comparison of voltage gain (G_V) of SSBB LED driver

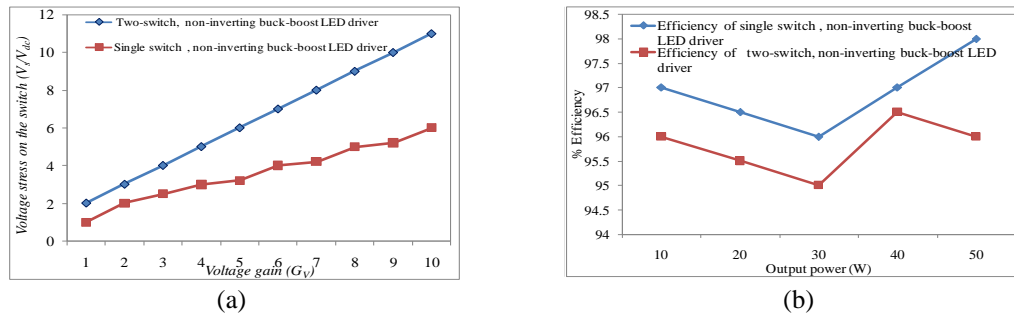| Parameters	Single switch converter-SSBB	Two switch converter [25]
Voltage gain (G_V)	$2d/(1-d)$	$d/(1-d)$
Voltage stress across the switch (S)	$Vs = (G_V + 2)/2V_{dc}$	$Vs = (G_V + 1)V_{dc}$

Figure 12. Performance analysis of SSBB LED driver with conventional buck-boost LED driver
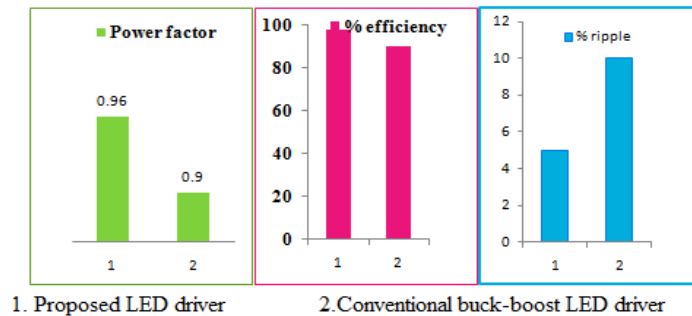(a) voltage stress comparison and (b) efficiency comparison

Figure 13. Comparison of SSBB LED driver with conventional buck-boost LED driver

6. CONCLUSION

A 50 W, SSBB converter used for high brightness LED lighting application is presented. The input PFC control scheme is implemented using ACMC. The PID controllers are tuned using ABC algorithm. By state space modelling of SSBB LED driver, the stability of the LED lighting system is investigated. The hardware implementation of ACMC is carried out by using PIC microcontroller (16F877A). The proposed SSBB LED driver provides an efficiency of 98% and it is compared with the state of art conventional buck-boost LED driver circuits.

REFERENCES

[1]   I. L. Azevedo, M. G. Morgan, and F. Morgan, "The transition to solid-state lighting," *Proceedings of the IEEE*, vol. 97, no. 3, pp. 481–510, Mar. 2009, doi: 10.1109/JPROC.2009.2013058.
[2]   Y. Gao, L. Li, K.-H. Chong, and P. K. T. Mok, "A hybrid LED driver with improved efficiency," *IEEE Journal of Solid-State Circuits*, vol. 55, no. 8, pp. 2129–2139, Aug. 2020, doi: 10.1109/JSSC.2020.2987730.
[3]   D. S. Ramchandra, M. S. Bhaskar, P. Sanjeevikumar, M. Mitolo, D. Almakhles, and J. B. Holm-Nielsen, "Study of basic units and simulation of passive light emitting diode (LED) driver configurations," in *2020 IEEE International Conference on Environment and Electrical Engineering and 2020 IEEE Industrial and Commercial Power Systems Europe (EEEIC / I&CPS Europe)*, Jun. 2020, pp. 1–6, doi: 10.1109/EEEIC/ICPSEurope49358.2020.9160821.
[4]   K. Saucke, G. Pausch, J. Stein, H.-G. Ortlepp, and P. Schotanus, "Stabilizing scintillation detector systems with pulsed LEDs: a method to derive the LED temperature from pulse height spectra," *IEEE Transactions on Nuclear Science*, vol. 52, no. 6, pp. 3160–3165, Dec. 2005, doi: 10.1109/TNS.2005.862929.
[5]   X. Qu, S.-C. Wong, and C. K. Tse, "Resonance-assisted buck converter for offline driving of power LED replacement lamps," *IEEE Transactions on Power Electronics*, vol. 26, no. 2, pp. 532–540, Feb. 2011, doi: 10.1109/TPEL.2010.2065242.
[6]   X. Liu, Y. Wan, Z. Dong, M. He, Q. Zhou, and C. K. Tse, "Buck–boost–buck-type single-switch multistring resonant LED driver with high power factor and passive current balancing," *IEEE Transactions on Power Electronics*, vol. 35, no. 5, pp. 5132–5143, May 2020, doi: 10.1109/TPEL.2019.2942488.
[7]   D. Venkatesh and S. V. Thazhathu, "Design and analysis of an integrated LC 3 –Valley fill passive LED driver," *International Journal of Electronics*, vol. 105, no. 12, pp. 2052–2065, Dec. 2018, doi: 10.1080/00207217.2018.1494331.
[8]   M. Schratz, C. Gupta, T. J. Struhs, and K. Gray, "A new way to see the light: improving light quality with cost-effective LED technology," *IEEE Industry Applications Magazine*, vol. 22, no. 4, pp. 55–62, Jul. 2016, doi: 10.1109/MIAS.2015.2459089.
[9]   C.-C. Chen, C.-Y. Wu, and T. F. Wu, "LED back-light driving system for LCD panels," in *Twenty-First Annual IEEE Applied Power Electronics Conference and Exposition, 2006. APEC '06.*, 2006, pp. 381–385, doi: 10.1109/APEC.2006.1620566.
[10] S. Li, S.-C. Tan, C. K. Lee, E. Waffenschmidt, S. Y. Hui, and C. K. Tse, "A survey, classification, and critical review of light-emitting diode drivers," *IEEE Transactions on Power Electronics*, vol. 31, no. 2, pp. 1503–1516, Feb. 2016, doi: 10.1109/TPEL.2015.2417563.
[11] S. Arulselvi, T. Archana, and G. Uma, "Design and implementation of CF-ZVS-QRC using analog resonant controller UC3861 for aerospace applications," in *2004 International Conference on Power System Technology, 2004. PowerCon 2004.*, 2004, vol. 2, pp. 1270–1275, doi: 10.1109/ICPST.2004.1460197.
[12] W.-Y. Choi and M.-K. Yang, "High-efficiency isolated SEPIC converter with reduced conduction losses for LED displays," *International Journal of Electronics*, vol. 101, no. 11, pp. 1495–1502, Nov. 2014, doi: 10.1080/00207217.2013.874044.
[13] U. R. Reddy and B. L. Narasimharaju, "Unity power factor buck-boost LED driver for wide range of input voltage application," in *2015 Annual IEEE India Conference (INDICON)*, Dec. 2015, pp. 1–6, doi: 10.1109/INDICON.2015.7443347.
[14] W.-H. Yang, H.-A. Yang, C.-J. Huang, K.-H. Chen, and Y.-H. Lin, "A high-efficiency single-inductor multiple-output buck-type LED driver with average current correction technique," *IEEE Transactions on Power Electronics*, vol. 33, no. 4, pp. 3375–3385, Apr. 2018, doi: 10.1109/TPEL.2017.2709039.
[15] M. J. Esfandani, M. Feizi, and R. Beiranvand, "CCM operation of a single-stage boost-flyback converter with active-clamp for LED driver applications," in *2020 11th Power Electronics, Drive Systems, and Technologies Conference (PEDSTC)*, Feb. 2020, pp. 1–6, doi: 10.1109/PEDSTC49159.2020.9088460.
[16] H.-C. Choi and H.-B. Shin, "A new soft-switched PWM boost converter with a lossless auxiliary circuit," *International Journal of Electronics*, vol. 93, no. 12, pp. 805–817, Dec. 2006, doi: 10.1080/00207210500491689.
[17] A. Shrivastava, B. Singh, and S. Pal, "A novel wall-switched step-dimming concept in LED lighting systems using PFC zeta converter," *IEEE Transactions on Industrial Electronics*, vol. 62, no. 10, pp. 6272–6283, Oct. 2015, doi: 10.1109/TIE.2015.2416338.
[18] A. Rahnamaee, J. Milimonfared, K. Malekian, and M. Abroushan, "Reliability consideration for a high power zero-voltage-switching flyback power supply," in *2008 13th International Power Electronics and Motion Control Conference*, Sep. 2008, pp. 365–371, doi: 10.1109/EPEPEMC.2008.4635292.
[19] B.-R. Lin and J.-J. Chen, "Analysis and implementation of active clamp SEPIC converter with synchronous rectifier," *International Journal of Electronics*, vol. 95, no. 12, pp. 1265–1278, Dec. 2008, doi: 10.1080/00207210802394094.
[20] B.-R. Lin, C.-L. Huang, and F.-P. Tsao, "Integrated Cuk-forward converter for photovoltaic-based LED lighting," *International*

Journal of Electronics, vol. 96, no. 9, pp. 943–959, Sep. 2009, doi: 10.1080/00207210902894761.

[21]   B.-R. Lin and C.-H. Tseng, "ZVS half-bridge SMPS design for LCD monitor and LCD-TV," *International Journal of Electronics*, vol. 96, no. 2, pp. 189–204, Feb. 2009, doi: 10.1080/00207210802387460.

[22]   P. Verma, N. Patel, N.-K. C. Nair, and A. Sikander, "Design of PID controller using cuckoo search algorithm for buck-boost converter of LED driver circuit," in *2016 IEEE 2nd Annual Southern Power Electronics Conference (SPEC)*, Dec. 2016, pp. 1–4, doi: 10.1109/SPEC.2016.7846102.

[23]   A. Jha and B. Singh, "Bridgeless buck-boost PFC converter for multistring LED driver," in *2017 IEEE Industry Applications Society Annual Meeting*, Oct. 2017, pp. 1–8, doi: 10.1109/IAS.2017.8101800.

[24]   Q. Cheng and H. Lee, "A high-frequency non-isolated ZVS synchronous buck-boost LED driver with fully-integrated dynamic dead-time controlled gate drive," in *2018 IEEE Applied Power Electronics Conference and Exposition (APEC)*, Mar. 2018, pp. 419–422, doi: 10.1109/APEC.2018.8341045.

[25]   U. R. Reddy and B. L. Narasimharaju, "Single-stage electrolytic capacitor less non-inverting buck-boost PFC based AC–DC ripple free LED driver," *IET Power Electronics*, vol. 10, no. 1, pp. 38–46, Jan. 2017, doi: 10.1049/iet-pel.2015.0945.

[26]   M. R. Banaei, H. Ardi, and A. Farakhor, "Analysis and implementation of a new single-switch buck–boost DC/DC converter," *IET Power Electronics*, vol. 7, no. 7, pp. 1906–1914, Jul. 2014, doi: 10.1049/iet-pel.2013.0762.

[27]   F. S. Abu-Mouti and M. E. El-Hawary, "Overview of artificial bee colony (ABC) algorithm and its applications," in *2012 IEEE International Systems Conference SysCon 2012*, Mar. 2012, pp. 1–6, doi: 10.1109/SysCon.2012.6189539.

[28]   K. Sundareswaran and V. T. Sreedevi, "Design and development of feed-back controller for a boost converter using a colony of foraging bees," *Electric Power Components and Systems*, vol. 37, no. 5, pp. 465–477, Apr. 2009, doi: 10.1080/15325000802599304.

[29]   K. Sundareswaran, V. Devi, S. K. Nadeem, V. T. Sreedevi, and S. Palani, "Buck-boost converter feedback controller design via evolutionary search," *International Journal of Electronics*, vol. 97, no. 11, pp. 1317–1327, Nov. 2010, doi: 10.1080/00207217.2010.488904.

[30]   H.-A. Ahn, S.-K. Hong, and O.-K. Kwon, "A highly accurate current LED lamp driver with removal of low-frequency flicker using average current control method," *IEEE Transactions on Power Electronics*, vol. 33, no. 10, pp. 8741–8753, Oct. 2018, doi: 10.1109/TPEL.2017.2783921.

[31]   M. G. Umamaheswari, G. Uma, and K. M. Vijayalakshmi, "Analysis and design of reduced-order sliding-mode controller for three-phase power factor correction using Cuk rectifiers," *IET Power Electronics*, vol. 6, no. 5, pp. 935–945, May 2013, doi: 10.1049/iet-pel.2012.0402.

[32]   S. Durgadevi and M. G. Umamaheswari, "Analysis and design of single phase power factor correction with DC–DC SEPIC converter for fast dynamic response using genetic algorithm optimised PI controller," *IET Circuits, Devices & Systems*, vol. 12, no. 2, pp. 164–174, Mar. 2018, doi: 10.1049/iet-cds.2017.0229.

[33]   M. Thirumeni and D. Thangavelusamy, "Design and analysis of hybrid PSO–GSA tuned PI and SMC controller for DC–DC Cuk converter," *IET Circuits, Devices & Systems*, vol. 13, no. 3, pp. 374–384, May 2019, doi: 10.1049/iet-cds.2018.5164.

BIOGRAPHIES OF AUTHORS

Devi Maheswaran 🆔 📇 SC ↻ is pursuing Ph.D. from Vellore Institute of Technology, Chennai. Her specialization includes LED drivers and Power converters. She is at present working as associate professor in the department of Rajalakshmi Engineering college Chennai. She has published papers in the area of power converters and presented papers in reputed international conferences related to LED drivers. She can be contacted at email: v.devi01123@gmail.com.

Sreedevi Vellithiruthi Thazhathu 🆔 📇 SC ↻ received her B.Tech. degree in Electrical Engineering from University of Calicut during 1988, Master of Technology in power systems and Ph.D. in power electronics from National Institute of Technology, Trichy, India. She is currently working as professor in the school of electrical Engineering, VIT, Chennai. Her research area includes DC-DC converters for renewable energy applications and LED drivers. She has published more than 40 journal publications and served as IEEE Power Electronics Society Chair, Madras Section, India. She can be contacted at email: sreedevi.vt@vit.ac.in.

Deepa Thangavelusamy 🆔 📇 SC ↻ has completed her B.E degree in Electrical and Electronics engineering from Manonmanium Sundaranar University, Tirunelveli, India, 1999, M.E degree in Power Systems from Anna University, Chennai, India 2007 and Ph.D. from Anna University, Chennai, India 2014. Working as an Associate Professor at, School of Electrical Engineering, VIT, Chennai. Her research area includes control system, intelligent controllers, fuzzy logic controller, sliding mode controller, optimization techniques, power electronics and electric vehicles; she published more than 40 conference and journal papers. The patent also published in the patent office journals. She can be contacted at email: deepa.t@vit.ac.in.